

Stereo Vision Based Digital Watermarking Using Regularized Feature-based Disparity Estimation

Kyung-Hoon Bae

Samsung Thales Company, Limited, San 14-1, Giheung-Gu, Yongin-City, Gyeonggi-Do, 446-712, Korea
E-mail: khbae.bae@samsung.com

Dong-Choon Hwang

Samsung Electronics Company, Limited, Yongtong-gu, Suwon-City, Gyeonggi-Do, 443-370, Korea

Eun-Soo Kim

3D Display Research Center (3DRC), Department of Electronic Engineering, Kwangwoon University,
Wolgye-Dong, Nowon-Gu, Seoul, 139-701, Korea

Abstract. This article proposes a stereo vision based digital watermarking scheme that uses regularized feature-based disparity estimation for copyright protection of stereo content. The watermark data are embedded into the right image of a stereo image using the discrete wavelet transform algorithm, and a disparity vector is extracted from the left and watermarked right images. The disparity vector and the left image are then transmitted to the recipient through a communication channel. At the receiver, the watermarked right image is reconstructed from the received left image and disparity vector by employing regularized feature-based disparity estimation. From the difference between the watermarked and original right images, the embedded watermark image can then be extracted. From experiments using the stereo image pair of "Fichier," "Tunnel," and watermark data of "3D," it was found that the peak signal to noise ratio (PSNR) of the reconstructed right image through the proposed algorithm can be improved by an average of 3.61 dB compared to those of a conventional algorithm. At the same time, the PSNR of the watermark image extracted from this reconstructed right image can also be improved by an average of 2.36 dB when the Quantizer Scale is given as 20. © 2008 Society for Imaging Science and Technology.

[DOI: 10.2352/J.ImagingSci.Technol.(2008)52:5(050503)]

INTRODUCTION

In general, the human visual system (HVS) reconstructs a three-dimensional (3D) world from the stereo pair of retinal images on a 3D display. Although the images on the retina are two-dimensional, what we see is typically 3D objects in a 3D space. Unquestionably, the human visual system succeeds in recovering the 3D scenes of the real world. Reconstruction of a 3D scene is known to be very difficult when using computer systems. Many vision scientists have investigated how the human visual system solves these problems. Thus far, great progress has been made regarding an understanding of what the HVS does to see the 3D real world.^{1,2}

The slight difference between the viewpoints of two eyes is known as the binocular disparity. This disparity gives ob-

jects a stereoscopic quality and through this, stereoscopic 3D image communication can be realized.³ A sequence of a stereo image pair, once received from a stereo camera system, is transmitted to a recipient through a channel. At the receiver, by projecting these stereo image pairs onto a specially designed screen, a stereoscopic 3D display can be achieved. However, a number of flaws can be found when using this technique in real applications. These include an increase of the signal bandwidth compared with that of a monocular image. Especially in the case of a multiview stereo image, the signal bandwidth can increase in proportion to the increased number of viewpoints; thus, development of an appropriate compression technique such as a disparity estimation scheme is necessary.⁴

Additionally, as computer networks and multimedia-related technologies are rapidly developing, it is inevitable that the demands for the use of stereoscopic 3D media through communication networks will increase tremendously. At the same time, this may increase the pirating of copyrighted materials as well. This has created a pressing need for a copyright control system that can unambiguously identify the copyright holder; accordingly, a number of copyright protection techniques under active development. Recently, digital watermarking⁵ was suggested as a new and strong means of the copyright protection of stereoscopic 3D digital media. Digital watermarking refers to the process of embedding particular information into the 3D digital content in an effort to protecting the copyright of the media. In this system, embedded data are always associated with the digital object to be protected or to the owner of the content. Additionally, disparity estimation (DE) can be considered as an extension of a motion estimation algorithm for the compression of video sequences. In the process of disparity estimation, many algorithms such as block-based disparity estimation (BDE) and feature-based disparity estimation (FDE) are now used for DE. Generally, BDE is a popular technique that estimates the degree of disparity on a block-by-block basis. BDE is known for its fast execution time; however, it is

Received Jan. 22, 2008; accepted for publication Jun. 6, 2008; published online Sep. 23, 2008.

1062-3701/2008/52(5)/050503/7/\$20.00.

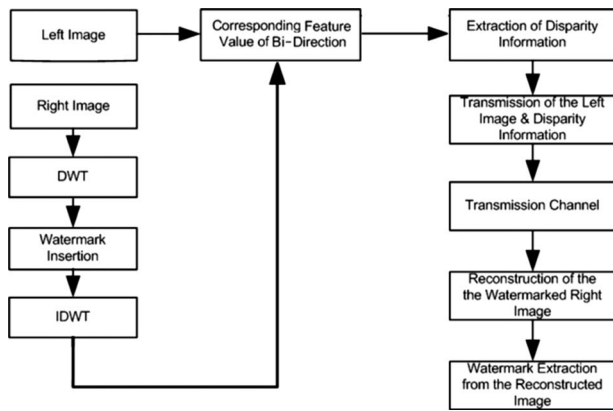


Figure 1. Flowchart of the proposed stereo image watermarking.

not known for particularly accurate (dense) matching. FDE has the capability of accurate matching at the edge of an object, but its overall execution time depends greatly on the characteristic of that images that are input into the system. With conventional disparity estimation, a matching window is fixed as a pixel or a block for input stereo images pair. However, it can be used more effectively in practical applications if a matching window is adaptively selected according to the feature values of an inputted stereo image pair. In this case, a smaller matching window is selected in a region with larger feature values while a larger matching window is taken in the region having feature values that are smaller than predetermined threshold values. In this approach, BDE and FDE are selectively and complementarily used in each local area depending on the specific feature values of input stereo image pairs, implying that the overall stereo matching performance can be expected to improve.

Therefore, in this article, a stereo-vision-based digital watermarking scheme using discrete wavelet transform⁶ (DWT) and regularized feature-based disparity estimation⁷ (RFDE) for copyright protection of stereo content is proposed. In the proposed approach, a watermark image is embedded into the right image of a stereo image pair via DWT and disparity information is extracted from this watermarked right image and from the left image. Both the left image and the disparity information are then transmitted to the recipient through the communication channel. At the receiver, the watermarked right image is reconstructed from the received left image and disparity data by employing RFDE. Finally, from the difference between the watermarked and original right images, the embedded watermark image can be extracted. The watermark extraction performance depends greatly on the employed wavelet transform and disparity matching algorithms; hence, using the stereo image pairs of “Fichier” and “Tunnel”, and a watermark image of “3D,” experiments on the extraction of the watermark from the right images as reconstructed by the RFDE and DWT were carried out and the performance was analyzed in terms of the peak signal to noise ratio (PSNR) of the extracted watermark image. These values were then compared with those of the disparity estimation and discrete cosine transform (DCT) algorithm.

WATERMARKING SCHEME IN STEREO VISION

Figure 1 shows a flowchart of the proposed digital watermarking scheme based on stereo vision using the DWT and RFDE algorithms. After the right image of a stereo image pair is transformed into the frequency domain, it is decomposed into three levels through the DWT. A watermark image is embedded into the middle-frequency band of the right image to achieve both perceptual invisibility and robustness to compression. The watermarked right image is finally generated through an I-DWT (inverse DWT) process of the watermarked DWT data.⁶ Disparity information between the watermarked right and left image is extracted using a bidirectional matching method, and this disparity information and the left image are transmitted to the recipient through the communication channel. At the receiver, the watermarked right image is reconstructed from both the received left image and disparity information using the RFDE algorithm, and a watermark image is finally extracted from this reconstructed right image.

In the stereo image communication that applies HVS, DE, and disparity compensation algorithms have been used to remove spatial redundancy. On the epipolar line, the relative displacement between two points corresponding to the left and right image of the same object is referred to as the binocular disparity. Its spatial vector representation is termed the disparity vector (DV). DE can simply be considered as an extension of motion estimation algorithms for the compression of video sequences.

Correspondence problems represent are among the most fundamental problems in stereo vision. The solution to a correspondence problem is a disparity vector through DE on the epipolar geometry. DE of correspondence in natural image pairs plays an important role in a large number of 3D applications such as 3D video processing, 3D conversions, and multiviewpoint image generation using intermediate view reconstruction.

The epipolar geometry places a very powerful restriction on correspondence with general validity. Figure 2 shows an example of the rectification process to transform the toed-in configuration to the parallel configuration. The captured stereo image is not on the same epipolar line in the toed-in configuration. However, this image can be made to be collinear to the same epipolar line through a rectification process. As a result, the corresponding point can be found on the same epipolar line. In Fig. 2, a point of the object is projected to the points of P_L and P_R of the left and right image planes through the respective lens center O_L , and O_R . Here, the plane joining the two lens centers O_L and O_R and a point is defined as the epipolar plane, and interactions of the epipolar plane are defined as the epipolar line, where C_L and C_R are the centers of the left and right planes, respectively. In principle, a correspondence problem determines the points of P_L and P_R in the left and right image planes that can be projected from the same point of $P(x, y, z)$ in 3D space, in which the difference between two points of P_L and P_R is known as the disparity value.

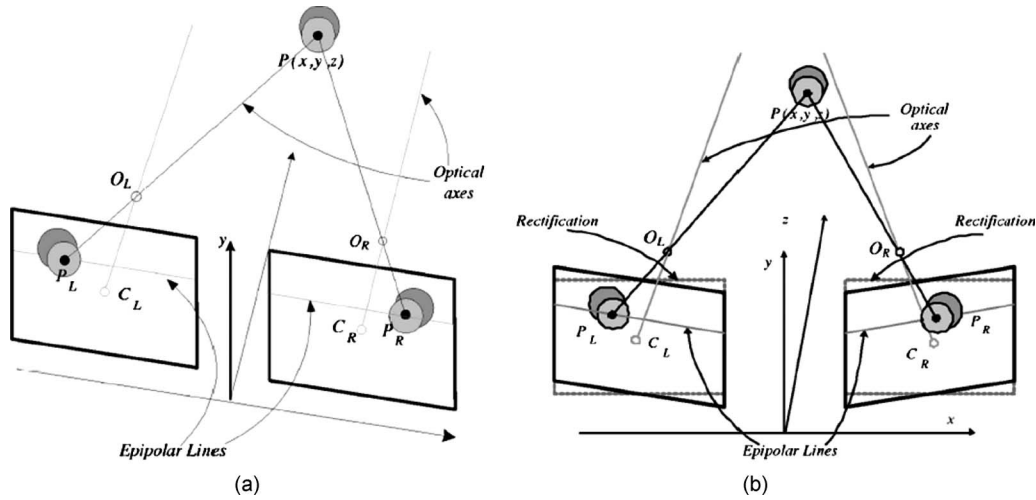


Figure 2. Epipolar geometry: (a) parallel and (b) toed-in stereoscopic camera configuration

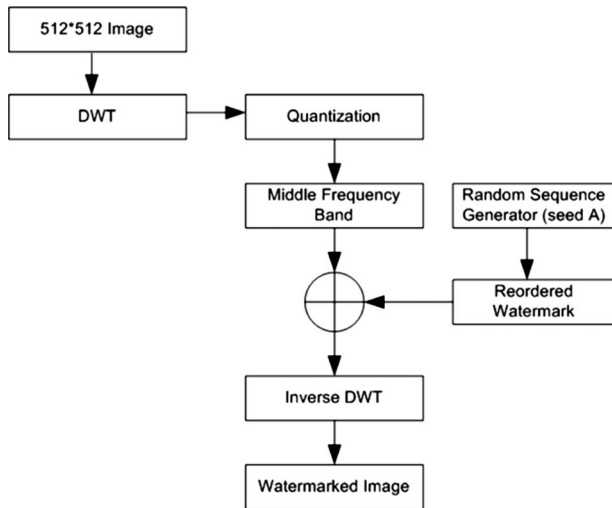


Figure 3. Block diagram of watermark embedding procedure.

Embedding Procedure of Watermark

Figure 3 shows the procedure of embedding the watermark to the stereo image via DWT. In this process, the right image of an original stereo image pair with 512×512 pixels is transformed into the frequency domain via DWT. The resultant DWT then consists of a set of the DWT coefficients.

The DWT coefficient of the right image of the original stereo image through three-level decomposition is given as Eq. (1),

$$f(t) = \sum_k c_j(k) \sqrt{2^j} \phi(2^j t - k) + \sum_k d_j(k) \sqrt{2^j} \psi(2^j t - k). \quad (1)$$

In the next step, these DWT coefficients are quantized using a quantization table and the results are given by the quantized DWT coefficient $F_q(u, v)$.

In general, when a watermark is embedded into the base band, in which most of the signal energy is converged, it is

possible either to have perceptual visibility or to distort the original image. On the other hand, a watermark embedded into the high-frequency band of an image can be easily eliminated with little degradation to the image via low-pass filtering. Accordingly, in this article, the watermark data are embedded into a middle frequency band as it is difficult to modify these coefficients sufficiently without violating fidelity. Moreover, this prevents the watermark from being eliminated by compression and cropping.^{8,9} The size of the watermark image is formed as 64×64 pixels, and these pixels are reordered using a random sequence generator so that the image has robustness against possible attacks on the domain or the areas. For synchronization between the encoder and the decoder without reference to the original image, the same seed is used at the encoder and the decoder to generate a random sequence, each element of which corresponds to one DWT coefficient.

The reordered watermark $X = \{x_1, x_2, \dots, x_K\}$ is embedded into the quantized DWT coefficients of the image $F_q(u, v) = \{t_1, t_2, \dots, t_L, \dots, t_M, \dots, t_N\}$. Among these values, each value x_i of the watermark is embedded into the corresponding coefficient range of $t_L - t_M$ according to the watermark embedding algorithm of Eq. (2). In this equation K represents the last pixel number of the watermark data and t_L and t_M denote the starting and finishing point, respectively, at which a watermark is embedded into the frequency value of $F_q(u, v)$. The symbol α is a proportionality factor that determines the PSNR and robustness of the watermarked image

$$t'_{L+i} = t_{L+i} + \alpha |t_{L+i}| X \quad (\text{where } i = 1, 2, \dots, M),$$

$$X = \{x_1, x_2, \dots, x_K\} \quad (\text{where } K = M - L). \quad (2)$$

If t_{L+i} , a part of the DWT coefficients of original right image, is replaced with t'_{L+i} , $F^*(u, v)$, the DWT coefficient corresponding to the watermarked one shown in Eq. (3). After obtaining $F^*(u, v)$ of the entire middle-frequency band, a watermarked image is finally generated by IDWT procedure, which is shown Eq. (4),

$$F^*(u, v) = \{t_1, t_2, \dots, t_L, t'_{L+1}, t'_{L+2}, \dots, t'_{L+N}, t_{L+N+1}, \dots, t_{64}\}, \quad (3)$$

$$c_{j+1}(k) = \sum_m c_j(m)h(k-2m) + \sum_m d_j(m)h_1(k-2m). \quad (4)$$

Extraction Process of Disparity Vector

Eq. (5) shows the MSE function used for extraction of the disparity vector from the input stereo image pair, where N_x and N_y represent the matching window size in the x and y directions, and $IL(i, j)$ and $IR(i+d, j)$ represent the left and right images in the coordinates of (i, j) and $(i+d, j)$, respectively,

$$MSE = \frac{1}{N_x N_y} \sum_{i=1}^{N_x} \sum_{j=1}^{N_y} |I_L(i, j) - I_R(i+d, j+l)|^2. \quad (5)$$

Eq. (6) shows the search area for extracting the disparity data, where $\pm S$ is a search range that is used to determine a corresponding block or pixel of the watermarked right image and both x_0 and y_0 indicate the starting point in the block of the left image when the DE process is performed,

$$S = \left\{ R(x, y) \left(x_0 - S_x + \frac{N_x}{2} \leq x \leq x_0 + S_x + \frac{N_x}{2} \right), \right. \\ \left. \left(y_0 \leq y \leq y_0 + \frac{N_y}{2} \right) \right\}. \quad (6)$$

Reconstructed Image by RFDE Algorithm

In this article, to reconstruct a watermarked right image from a received left image and from the disparity information, the RFDE algorithm is employed.^{7,10} During the reconstruction process of the right image, the appearance of several occluded regions, which one of the stereo cameras sees while the other does not, can occur. As the disparity vector is not allocated to this occluded region, the average value of the disparities of the nearby regions is assigned through the process of disparity stability. If the positions of the area are not occluded, the disparity is defined as the difference between the positions of the image points in the two images. Eq. (7) shows the disparity in the horizontal direction and the relationship between the right image I_r and the left image I_l ,

$$I_r = \begin{bmatrix} i_r \\ j_r \end{bmatrix} = \begin{bmatrix} i_l + DV(i_l, j_l) \\ j_l \end{bmatrix} = I_l + \begin{bmatrix} DV(i_l, j_l) \\ 0 \end{bmatrix}. \quad (7)$$

Thus, in the RFDE algorithm, the matching window size is adoptively determined depending on the feature value of the input stereo image. From this process of disparity matching, the watermarked right image is reconstructed.

Regularized Disparity Estimation Algorithm

In this article, a regularized DE algorithm employing a neighborhood averaging-based regularization scheme is used for alleviating the problems of matching window overlapping and misallocation occurring in the conventional feature-based disparity estimation. Here, the regularized pixel $g(x, y)$ is defined by Eq. (8),

$$g(x, y) = \frac{1}{M} \sum_{(i,j) \in S} f(i, j), \quad (8)$$

where M and S are the number and set of neighborhood pixels $(i \times j)$, respectively. Eq. (9) is used to preserve the edge value in an edge region,

$$g(x, y) = \begin{cases} \frac{1}{M} \sum_{(m,n) \in S} f(m, n) & \text{if } |f(x, y) - \sum_{(m,n) \in S} \left| \frac{1}{M} f(m, n) \right| < T \\ f(x, y) & \text{otherwise.} \end{cases} \quad (9)$$

If the difference between the regularized and original pixel value $f(x, y)$ is smaller than a predetermined threshold, the original pixel value is replaced with the regularized value. Otherwise, problems of over regularization can be solved through the use of the original pixel value. The threshold value used in this algorithm is determined by finding edges through a Laplacian operation and then by choosing the points whose disparity gradients are larger than a certain threshold.

Accordingly, in this article, the disparity is estimated through an adaptive matching process using an edge preserving regularization scheme with a threshold. In this scheme, matching windows are adaptively selected in accordance with the magnitudes of the extracted feature values from the input stereo images pair. However, the adaptive selection of matching windows can lead to overlapping and misallocation of the disparity vectors in some areas; therefore, in the proposed method, disparity vectors of those regions are regularized with the mean values of the disparity vectors of a nearby region. With this regularization process, more effective reconstruction of the predicted stereo images is expected.

During the reconstruction process of the right image, a number of occluded regions may emerge that one of the stereo cameras sees while the other does not. As a disparity vector is not allocated to this occluded region, the average value of the disparities of nearby regions is assigned through the process of disparity stability. If the viewpoint is not occluded, the disparity is then defined as the distance between the image points in both images. Eq. (10) shows the disparity in the horizontal direction and the relationship between the right image I_r and left image I_l ,

$$I_r = \begin{bmatrix} i_r \\ j_r \end{bmatrix} = \begin{bmatrix} i_l + DV(i_l, j_l) \\ j_l \end{bmatrix} = I_l + \begin{bmatrix} DV(i_l, j_l) \\ 0 \end{bmatrix}. \quad (10)$$

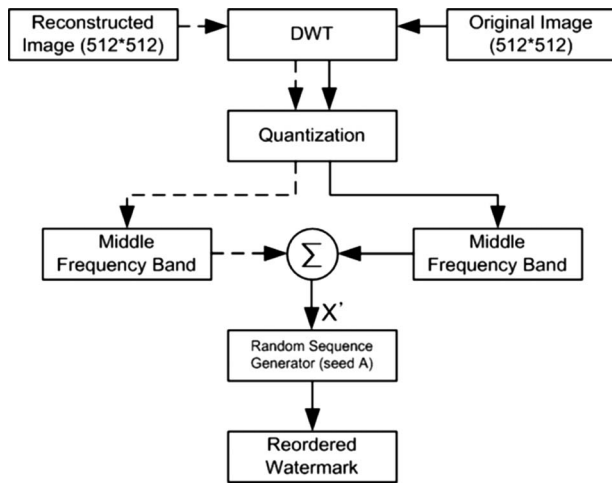


Figure 4. Block diagram of a watermark extraction procedure.

Extraction of Watermark From the Reconstructed Stereo Image

Figure 4 shows the extraction procedure of a watermark from a reconstructed right image.

First, the original right image of 512×512 pixels is decomposed into three levels by DWT. Through a quantization operation, the quantized DWT coefficient of $F_q(u, v)$ can be derived. Likewise, the watermarked right image reconstructed from the left image and disparity data using the RFDE algorithm, is also transformed into the frequency domain through the DWT, and is quantized to $F^{**}(u, v)$. Given that the watermark data is directly added to the DWT coefficients of the middle frequency components, the embedded watermark image X' can be extracted by subtracting $F^{**}(u, v)$ from $F_q(u, v)$. Moreover, as the extracted watermark data X' consists of randomly reordered values that were generated in the process of the embedding of the watermark with a random sequence, the same seed value used in the embedding process must be applied to the random sequence generator to obtain a final watermark image.

EXPERIMENTAL RESULTS AND ANALYSIS

In the experiments, the stereo image pairs of the words “Fichier” and “Tunnel” was used as a cover image. First, it was transformed into a “raw” file of 512×512 pixels. The DISTIMA project image sequences of “Fichier” and “Tunnel” were captured courtesy of Commun D’Etudes de Telediffusion et Telecommunications. This set of sequences is regarded as a standard in the stereoscopic sequence compression community. In addition, the lettering of 3D at a resolution of 64×64 pixels was also used as a watermark image, as shown in Figure 5. Computer simulation was performed using “Microsoft Visual Studio 6.0.” In the experiment, the performance of the process of extracting the watermark images was analyzed in terms of PSNR when right images were reconstructed from the proposed algorithm and when the seed value was fixed to be 20. These results were then compared to those obtained using a conventional algorithm.

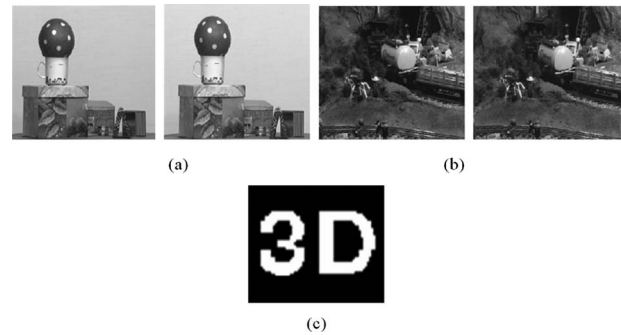


Figure 5. Stereo image pair of (a) Fichier, (b) Tunnel, and (c) watermark image of 3D.

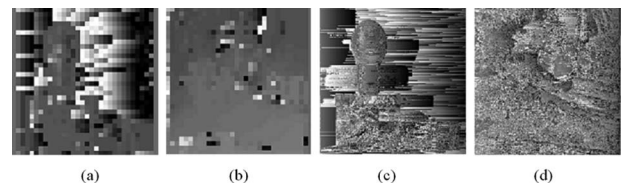


Figure 6. Disparity maps: (a) 8×8 BDE of Fichier, (b) 8×8 BDE of Tunnel, (c) RFDE of Fichier, and (d) RFDE of Tunnel.

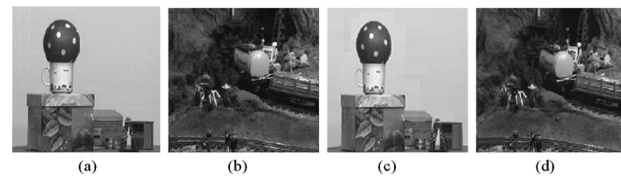


Figure 7. Reconstructed right image: (a) 8×8 BDE of Fichier, (b) 8×8 BDE of Tunnel, (c) RFDE of Fichier, and (d) RFDE of Tunnel.

Figure 6 shows disparity maps extracted using the block-based disparity BDE and RFDE algorithms. Figs. 6(a) and 6(b) show 8×8 block-based disparity maps of “Fichier” and “Tunnel”, and Figs. 6(c) and 6(d) show feature-based disparity maps of “Fichier” and “Tunnel”, respectively.

Figure 7 shows a reconstructed right image using each matching algorithm. Figs. 7(a) and 7(b) show the reconstructed right images of “Fichier” and “Tunnel” using 8×8 BDE, respectively, and Figs. 7(c) and 7(d) show reconstructed right images of “Fichier” and “Tunnel” using RFDE, respectively.

In the present work, the DWT algorithm was used to embed the watermark into the cover image. In this process, the right image of “Fichier” and “Tunnel” were decomposed into wavelet subimages via level-3 dyadic DWT. Here, a part of the middle frequency band was cast due to its inconspicuousness and robustness against image processing algorithms. To heighten its robustness against attacks, the watermark

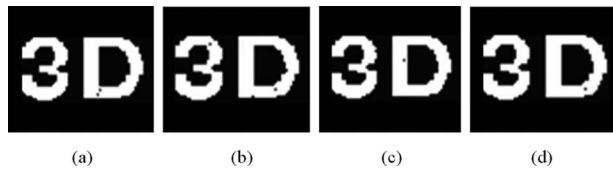


Figure 8. Extracted watermark images from reconstructed right image of Fichier (a), BDE and DCT (b), BDE and DWT (c), RFDE and DCT (d), and the proposed algorithm.

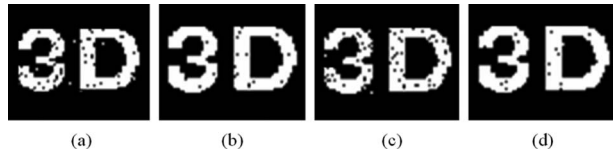


Figure 9. Extracted watermark images with the blurred reconstruction images from reconstructed right image of Fichier (a), BDE and DCT (b), BDE and DWT (c), RFDE and DCT (d), and the proposed algorithm.

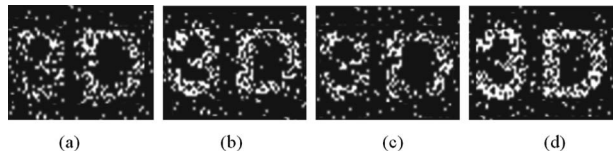


Figure 10. Extracted watermark images with Gaussian noises from reconstructed right image of Fichier (a), BDE and DCT (b), BDE and DWT (c), RFDE and DCT (d), and the proposed algorithm.

data were rearranged in a random sequence before it was embedded. In this article, the seed value was determined to be 20.

Figure 8 also shows the watermark images extracted from the reconstructed right image using the BDE and DCT, BDE and DWT, RFDE and DCT, and the proposed algorithm.

Figure 9 shows blurred disparity maps and watermark images extracted using the processes of the watermark data extraction via BDE and DCT, BDE and DWT, RFDE and DCT, and the proposed algorithm.

Figure 10 shows disparity maps with Gaussian noise along with the watermark data extracted from these maps. In this case, the image quality of the extracted watermark data were found to be less than ideal when extracted via BDE and DCT, BDE and DWT, RFDE and DCT, and the proposed algorithm.

Table I shows the calculated PSNR values of images reconstructed using the BDE and DCT, BDE and DWT, RFDE and DCT, and the proposed algorithm for the “Fichier” and “Tunnel” watermarks under three types of attacks. Table II shows the calculated PSNR values of the watermark images extracted from reconstructed right images

Table I. PSNR comparison of the reconstructed right image under some attacks.

Reconstructed right image	Algorithm	PSNR (dB)		
		General	Blurring	Gaussian noise
Fichier	BDE and DCT	27.3	24.6	23.2
	BDE and DWT	28.9	25.2	24.1
	FDE and DCT	30.2	28.4	27.5
	The proposed algorithm	32.6	29.7	28.6
Tunnel	BDE and DCT	26.2	23.6	22.5
	BDE and DWT	27.4	24.2	23.8
	FDE and DCT	29.1	26.4	26.2
	The proposed algorithm	30.7	28.3	27.8

Table II. PSNR comparison of the extracted watermark image under some attacks.

Reconstructed watermark image	Algorithm	PSNR (dB)		
		General	Blurring	Gaussian noise
3D (Fichier)	BDE and DCT	14.2	6.2	5.7
	BDE and DWT	15.2	6.9	6.1
	FDE and DCT	19.2	8.3	7.5
	The proposed algorithm	21.4	8.7	8.2
3D (Tunnel)	BDE and DCT	13.1	5.3	5.1
	BDE and DWT	14.2	6.1	5.8
	FDE and DCT	18.8	7.2	6.8
	The proposed algorithm	20.7	7.8	7.5

reconstructed by the BDE and DCT, BDE and DWT, RFDE and DCT, and the proposed algorithm for “Fichier” and “Tunnel” under three types of attacks. From Table I, it can be observed that the PSNR of the right image reconstructed using the proposed algorithm is improved by 3.61 dB on average compared to the PSNR of the conventional algorithm. Moreover, the PSNR of the watermark image as ex-

tracted from this reconstructed right image is also improved by 2.36 dB on average when the seed value is 20, as shown in Table II.

CONCLUSION

In this article, a digital watermarking scheme based on a stereo vision system that can be used for the copyright protection of stereo content is proposed and its performance is evaluated in terms of the PSNR values of the extracted wa-

termark data. From experiments using the stereo image pair of “Fichier” and “Tunnel” and the watermark data of 3D, it was found that the PSNR of the reconstructed right image through the proposed algorithm can be improved by 3.61 dB on average compared to these values obtained using a conventional algorithm. In addition, the PSNR of the watermark image extracted from this reconstructed right image showed improvement of 2.36 dB on average when the seed value is set to 20.

REFERENCES

- ¹I. Howard and B. Rogers, *Binocular Vision and Stereopsis* (Oxford University Press, Oxford, 1995).
- ²S. T. Barnard and W. B. Thompson, “Disparity analysis of image”, *IEEE Trans. Pattern Anal. Mach. Intell.* **2**, 333–340 (1980).
- ³J. R. Ohm and K. Muller, “Incomplete 3D multiview representation of video objects”, *IEEE Trans. Circuits Syst. Video Technol.* **9**, 389–400 (1999).
- ⁴A. Redert, E. Hendriks, and J. Biemond, “Correspondence estimation in image pairs”, *IEEE Signal Process. Mag.* **16**, 29–46 (1999).
- ⁵I. J. Cox, J. Kilian, T. Leighton, and T. Shamoan, “Secure spread spectrum watermarking for multimedia”, *IEEE Trans. Image Process.* **6**, 1673–1687 (1997).
- ⁶Y. Wang, J. F. Doherty, and R. E. van Dyck, “A wavelet-based watermarking algorithm for ownership verification of digital image”, *IEEE Trans. Image Process.* **11**, 77–88 (2002).
- ⁷K. H. Bae, J. J. Kim, and E. S. Kim, “A new disparity estimation scheme based-on adaptive matching window for intermediate-view reconstruction”, *Opt. Eng. (Bellingham)* **42**, 1778–1786 (2003).
- ⁸C. S. Lu, “Block DCT-based robust watermarking using side information extracted by mean filtering”, *Proceedings, 16th International Conference on Pattern Recognition*, Vol. **2**, 2002, pp. 1001–1004.
- ⁹D. Zheng, Y. Liu, and Jiying Zhao, “RST rnvriant digital image watermarking based on a new phase-only filtering method”, *Signal Process.* **85**, 2354–2370 (2005).
- ¹⁰K. H. Bae, J. H. Ko, and J. S. Lee, “Regularized stereo matching scheme using adaptive disparity estimation”, *Jpn. J. Appl. Phys., Part 1* **45**, 4107–4115 (2006).